

# Reconfigurable frequency-modulated microwave generation using multi-wavelength optically injected semiconductor laser

Xiaoyue Yu

Nanjing University of Aeronautics and  
Astronautics, Nanjing, China  
Wuhan National Laboratory for  
Optoelectronics, Wuhan, China  
yuxiaoyue@nuaa.edu.cn

Fangzheng Zhang

Nanjing University of Aeronautics and  
Astronautics, Nanjing, China  
Wuhan National Laboratory for  
Optoelectronics, Wuhan, China  
zhangfangzheng@nuaa.edu.cn

Boyang Wu

Nanjing University of Aeronautics and  
Astronautics, Nanjing, China  
Wuhan National Laboratory for  
Optoelectronics, Wuhan, China  
wuby@nuaa.edu.cn

Guanqun Sun

Nanjing University of Aeronautics and  
Astronautics, Nanjing, China  
Wuhan National Laboratory for  
Optoelectronics, Wuhan, China  
sunguanqun@nuaa.edu.cn

Shilong Pan

Nanjing University of Aeronautics and  
Astronautics, Nanjing, China  
Wuhan National Laboratory for  
Optoelectronics, Wuhan, China  
pans@nuaa.edu.cn

Xinyi Li

Nanjing University of Aeronautics and  
Astronautics, Nanjing, China  
Wuhan National Laboratory for  
Optoelectronics, Wuhan, China  
lixinyi@nuaa.edu.cn

**Abstract**—A method for photonic generation of frequency modulated microwave signals is demonstrated based on period-one (P1) dynamics under multi-wavelength optical injection in a semiconductor laser. By properly setting the wavelengths and power of the optical injection signal, microwave signals with reconfigurable frequency modulation profiles can be generated. Feasibility of the proposed method is verified through both simulation and experiments, in which microwave signals with dual-chirp linear frequency modulation, cosine profile frequency modulation, Gaussian pulse profile modulation and square profile frequency modulation are generated. The proposed method is a promising solution to generating reconfigurable waveforms for radar, communication and electronic warfare applications.

**Keywords**—Frequency modulation, microwave photonics, optical injection, semiconductor laser

## I. INTRODUCTION

Microwave waveform generators are important components in radar, communication and electronic warfare systems [1, 2]. In recent years, microwave photonic techniques have been widely investigated as a promising solution to improve the bandwidth and performance of traditional electrical signal generators [3-6]. Among these methods, microwave signal generation based on period one (P1) oscillation in an optically injected semiconductor laser is of particular interest, which features optical controllability, compact structure and wide frequency tunability. The P1 oscillation frequency increases approximately linearly as the increase of injection strength at a fixed detuning frequency, and the generated signals cover a large frequency range from a few GHz to over 100 GHz [7]. The characteristics of signal generation based on P1 dynamics under single-wavelength optical injection have been intensively investigated [8-9]. For example, in [8], an electrical control signal is applied to an intensity modulator to manipulate the injection strength, through which frequency-modulated (FM) microwave signals with a large time-

bandwidth product are generated. However, the investigation of P1 dynamics with multi-wavelength optical injection is rarely reported. In our previous work, a scheme of FM signal generation by dual-wavelength injection P1 laser dynamics is demonstrated [10]. This method has a compact structure and high stability without using external modulators and electrical driving signal generators, but the generated signals have a fixed frequency modulation characteristics with a cosine profile.

In this paper, we extend the previous work and investigate the P1 oscillation under multi-wavelength injection, through which microwave signals with reconfigurable FM profiles can be generated by choosing proper injection parameters including the wavelengths and power of the optical injection signal. The dynamic characteristics of multi-wavelength optical injection are numerically investigated using the modified laser nonlinear rate equations. The generation of microwave signals with several typical frequency modulation profiles including dual-chirp linear frequency modulation, cosine profile frequency modulation, Gaussian pulse profile modulation and square profile frequency modulation are demonstrated through simulation and experiment.

## II. PRINCIPLE

Fig.1 shows the schematic diagram of the proposed multi-wavelength optically injected semiconductor laser.  $N$  master lasers (MLs) with different frequencies ( $f_1, f_2, \dots, f_N$ ) are combined by an optical coupler (OC) and then injected into the slave laser (SL) simultaneously via an optical circulator (CIR). The SL is a semiconductor laser with a free-running frequency of  $f_s$ . Before injected to the SL, multiple polarization controllers (PCs) are used to align the polarization states of the injected light beams with that of the SL to maximize the injection efficiency and multiple optical attenuators (ATTs) are used to adjust the optical injection power. To excite P1 oscillation, the detuning frequency and injection strength of each ML need to be carefully adjusted. Here, the injection strength of each ML is defined as the square root of its power divided by the output power of the free-running SL and the detuning frequency is defined as the frequency difference of each ML and the free-running SL. In single-wavelength optical injection, the optical power injected

This work was supported by the National Key Research and Development Program of China (2021YFB2800803), the Natural Science Foundation of Jiangsu Province (BK20221479), the Open Project Program of Wuhan National Laboratory for Optoelectronics (2022WNLOKF002), the Open Fund of State Key Laboratory of Advanced Optical Communication Systems and Networks (2023GZKF03) and the Fund of Prospective Layout of Scientific Research for NUA.

to the SL is constant. The output optical signal from the SL contains a regenerated optical carrier and a red-shifted cavity mode generated via the anti-guidance effect [11]. The P1 oscillation frequency is fixed and a single-frequency microwave signal is obtained after optical-to-electrical conversion. For the proposed multi-wavelength injection system, the output optical signal from the SL contains multiple regenerated optical carriers, a frequency-swept red-shifted cavity mode at  $f_s'$  and four-wave mixing idlers (FWM). The power beating between the regenerated carriers result in equivalent amplitude modulation of the optical power injected to the SL and the P1 oscillation frequency is changed accordingly. To remove the FWM idlers, an optical band-pass filter (OBPF) is followed, and the output signal is sent to a photodetector (PD) to complete optical-to-electrical conversion. By choosing the multiple injection wavelengths to get proper detuning frequencies, and by adjusting the power of each ML to control the injection strength, an FM microwave signal with arbitrary frequency modulation profile can be generated.

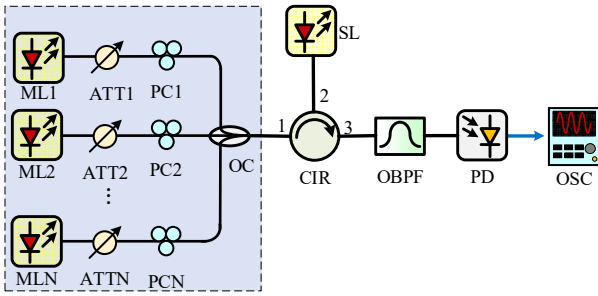


Figure 1. Schematic diagram of the proposed multi-wavelength optically injected semiconductor laser system. ML, master laser; ATT, attenuator; PC, polarization controller; OC, optical coupler; CIR, optical circulator; SL, slave laser; OBPF, optical band-pass filter; PD, photodetector, OSC, oscilloscope.

### III. SIMULATION AND EXPERIMENTAL RESULTS

To investigate the performance of the proposed method, numerical simulations are conducted by solving the modified laser nonlinear rate equations under multi-wavelength optical injection, which are expressed as

$$\frac{da_r}{dt} = \frac{1}{2} \left[ \frac{\gamma_n \gamma_c}{\gamma_s \tilde{J}} \tilde{n} - \gamma_p (a_r^2 + a_i^2 - 1) \right] (a_r + b a_i) + \xi_1 \gamma_c \cos(2\pi f_{i1} t) + \xi_2 \gamma_c \cos(2\pi f_{i2} t) + \dots + \xi_N \gamma_c \cos(2\pi f_{iN} t) \quad (1)$$

$$\frac{da_i}{dt} = \frac{1}{2} \left[ \frac{\gamma_n \gamma_c}{\gamma_s \tilde{J}} \tilde{n} - \gamma_p (a_r^2 + a_i^2 - 1) \right] (-b a_r + a_i) - \xi_1 \gamma_c \sin(2\pi f_{i1} t) - \xi_2 \gamma_c \sin(2\pi f_{i2} t) - \dots - \xi_N \gamma_c \sin(2\pi f_{iN} t) \quad (2)$$

$$\frac{d\tilde{n}}{dt} = -[\gamma_s + \gamma_n (a_r^2 + a_i^2)] \tilde{n} - \gamma_s \tilde{J} (a_r^2 + a_i^2 - 1) + \frac{\gamma_s \gamma_p}{\gamma_c} \tilde{J} (a_r^2 + a_i^2) (a_r^2 + a_i^2 - 1) \quad (3)$$

where  $a_r$  and  $a_i$  are real and imaginary parts of the normalized total complex intracavity field amplitude at the oscillation frequency, and  $\tilde{n}$  is the normalized charge carrier density. The laser intrinsic parameters  $\gamma_c$ ,  $\gamma_n$ ,  $\gamma_s$ ,  $\gamma_p$ ,  $b$ , and  $\tilde{J}$  are the cavity decay rate, differential carrier relaxation rate, spontaneous carrier relaxation rate, nonlinear carrier relaxation rate, linewidth enhancement factor and normalized current above threshold, respectively. In addition,  $\xi_N$  and  $f_{iN}$  are the injection strength and detuning frequency of the  $N$ -th ML, respectively. The frequency difference between the  $M$ -th ML and the  $N$ -th ML is defined as  $\Delta f_{MN}$  ( $\Delta f_{MN} = f_N - f_M$ ). In our simulation, the

intrinsic parameters are  $\gamma_c = 5.36 \times 10^{11} \text{ s}^{-1}$ ,  $\gamma_n = 7.53 \times 10^9 \text{ s}^{-1}$ ,  $\gamma_s = 5.96 \times 10^9 \text{ s}^{-1}$ ,  $\gamma_p = 1.91 \times 10^{10} \text{ s}^{-1}$ ,  $b = 3.2$ , and  $\tilde{J} = 1.222$  [12]. The relaxation resonance frequency of the SL is about 10.25 GHz. In the analysis, the fourth-order Runge-Kutta algorithm is used to solve Eqs. (1)-(3) with a temporal step of 0.25 ps within a period of 0.1  $\mu\text{s}$ .

First, the generation of a dual-chirp linear frequency modulation (LFM) signal under three-wavelength injection is demonstrated, with the results shown in Fig. 2. The injection parameters including the detuning frequencies and injection strengths are  $(f_{i1}, \xi_1) = (5 \text{ GHz}, 0.15)$ ,  $(f_{i2}, \xi_2) = (5.2 \text{ GHz}, 0.025)$  and  $(f_{i3}, \xi_3) = (5.6 \text{ GHz}, 0.0028)$ . Fig. 2(a) is the optical spectrum at the output of the SL, in which the regenerated optical carriers, the frequency-swept red-shifted sideband and the FWM idlers are observed. Fig. 2(b) shows the time domain waveform of the generated dual-chirp LFM signal. Fig. 2(c) shows the electrical spectrum of the generated FM signal, and Fig. 2(d) shows the instantaneous frequency recovered by performing short-time Fourier transform. A dual-chirp LFM signal is generated containing an up-chirp and a down-chirp covering a bandwidth of 4.6 GHz (17.56-22.16 GHz). The temporal period is found to be 5 ns, which equals the reciprocal of the frequency difference  $\Delta f_{12}$  between ML1 and ML2. Here, the amplitude of generated signal fluctuates slightly, which is mainly caused by the dynamic competition between the red-shifted cavity resonance mode and the multiple regenerated optical carriers. In practical applications, this problem can be solved by using electrical and optical power limiting techniques [13].

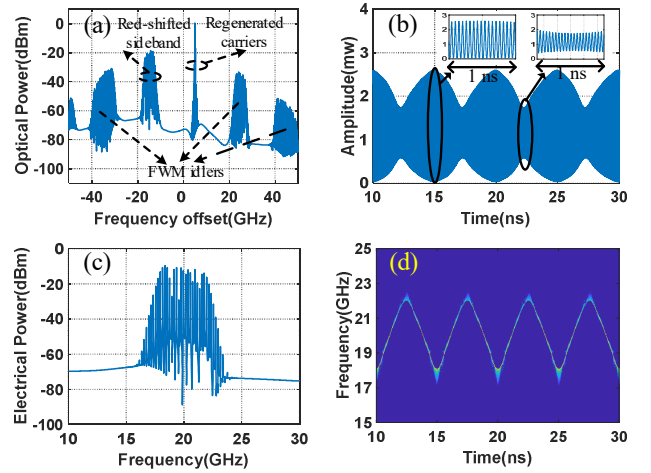


Figure 2. Simulation results for generating a dual-chirp LFM signal with a bandwidth of 4.6 GHz (17.56-22.16 GHz): (a) optical spectrum at the output of SL, (b) the time domain waveform, (c) the electrical spectrum, and (d) the recovered instantaneous frequency.

In the simulation, the generation of FM signals with other profiles are also achieved, with their waveforms and instantaneous frequencies shown in Fig. 3. Figs. 3(a-i) and (a-ii) show the results of generated signal having a cosine FM profile under dual-wavelength optical injection with the injection parameters of  $(f_{i1}, \xi_1) = (5 \text{ GHz}, 0.15)$  and  $(f_{i2}, \xi_2) = (5.2 \text{ GHz}, 0.025)$ . Fig. 3(b-i) and (b-ii) show the results of generated signal having a Gaussian pulse FM profile, achieved under four-wavelength injection with the injection parameters of  $(f_{i1}, \xi_1) = (5 \text{ GHz}, 0.15)$ ,  $(f_{i2}, \xi_2) = (5.2 \text{ GHz}, 0.025)$ ,  $(f_{i3}, \xi_3) = (5.4 \text{ GHz}, 0.0125)$  and  $(f_{i4}, \xi_4) = (5.6 \text{ GHz}, 0.0031)$ . Fig. 3(c-i) and (c-ii) show the FM signal with square

profile under four-wavelength when injection parameters are set as  $(f_{i1}, \xi_1) = (5 \text{ GHz}, 0.15)$ ,  $(f_{i2}, \xi_2) = (5.2 \text{ GHz}, 0.025)$ ,  $(f_{i3}, \xi_3) = (5.6 \text{ GHz}, -0.0083)$  and  $(f_{i4}, \xi_4) = (6 \text{ GHz}, 0.005)$ . These results show the capability of generation FM signals with different profiles using the multi-wavelength injection system.

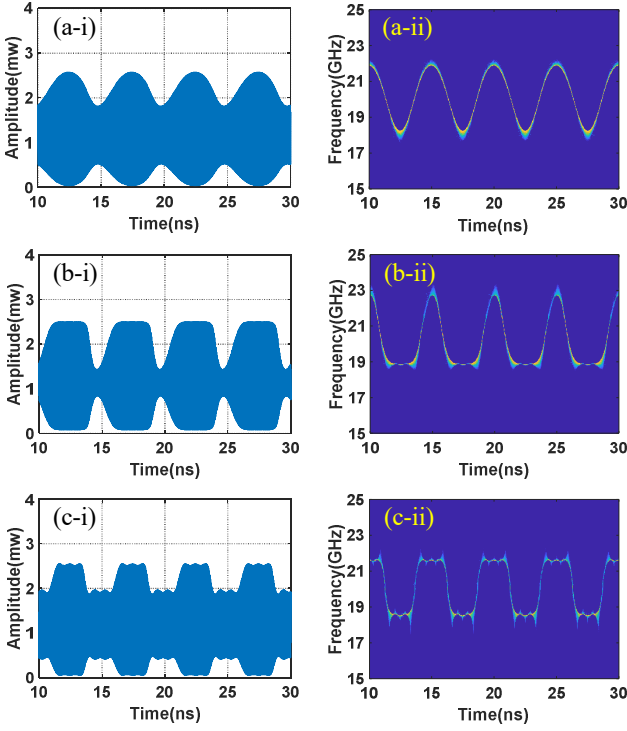


Figure 3. (i) The time domain waveform and (ii) the recovered instantaneous frequency results for generating FM signals with other profile: (a) cosine, (b) Gaussian pulse, and (c) square profile.

To further investigate the performance of the proposed method, proof-of-concept experiments are conducted based on the setup in Fig.1. Firstly, a microwave signal with cosine FM profile is generated under dual-wavelength optical injection. In the experimental demonstration, a commercial distributed feedback semiconductor laser (Actech LD15DM) is applied as the SL. The free-running wavelength of the SL is 1542.056 nm and its output power is 7.53 dBm when the bias current is 59.9 mA. The ML1 (Cobrite) has a wavelength of 1542.045 nm and its output power is 9 dBm. ML2 is a tunable narrow linewidth laser (TeraXion, PS-NLL- 1550.12-040) of which the wavelength is tuned to 1542.0432 nm, and its output power is 5 dBm. The corresponding injection parameters are:  $(f_{i1}, \xi_1) = (1.388 \text{ GHz}, 1.184)$  and  $(f_{i2}, \xi_2) = (1.615 \text{ GHz}, 0.747)$ . Fig. 4(a) show the optical spectrum of the MLs and SL at the free-running state, which is measured by an optical spectrum analyzer (Yokogawa AQ6370D) with a resolution of 0.02 nm. After optical injection, the optical spectrum at the output of the SL is measured, which consists of the regenerated optical carriers, the frequency-swept red-shifted sideband and other FWM idler components, as shown in Fig. 4(b). Then, the regenerated optical carriers and the frequency-swept red-shifted sideband are selected by an OBPF (Yenista XTM-50). The obtained signal spectrum after OBPF is also shown in Fig. 4(b). After optical-to-electrical conversion at a PD (u2t XPDV2120RA) with a bandwidth of 40 GHz, a microwave signal with a cosine FM profile is generated, and the generated FM microwave signal is sampled by a real-time oscilloscope (OSC, Tektronix DSA72004B)

with a sampling rate of 50 GSa/s. Fig. 5(a) shows the measured waveform of the generated signal and Fig. 5 (b) shows the recovered instantaneous frequency. As can be seen, the generated signal has a bandwidth of 6.75 GHz (12-18.75 GHz) and a temporal period of 4.4 ns.

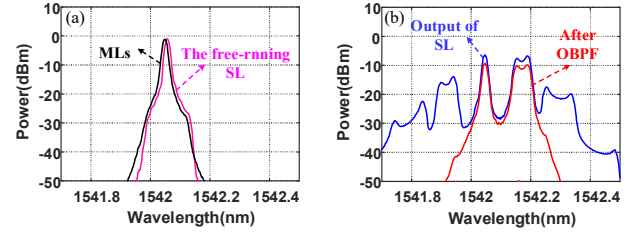


Figure 4. Measured optical spectra of (a) the free-running SL and the MLs, (b) the signal after optical injection and the signal after OBPF when the number of MLs is 2 and the injection parameters are  $(f_{i1}, \xi_1) = (1.388 \text{ GHz}, 1.184)$  and  $(f_{i2}, \xi_2) = (1.615 \text{ GHz}, 0.747)$ .

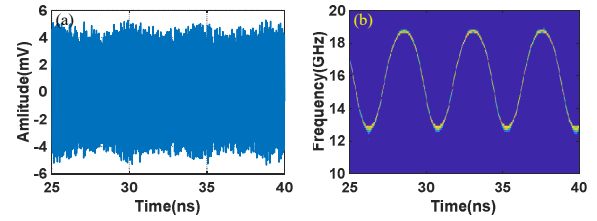


Figure 5. (a) Measured temporal waveform of the generated cosine FM signal with a bandwidth of 6.75 GHz (12-18.75 GHz), and (b) its instantaneous frequency.

Finally, the generation of a dual-chirp LFM microwave signal is demonstrated under three-wavelength optical injection. When the bias current is 36.8 mA and the thermistor resistance is 4.487 k $\Omega$ , the free-running wavelength and output power of the SL are 1543.406 nm and 6.30 dBm, respectively. In the experiment, three MLs generated by a multi-channel laser source (Agilent N7714A) are used. The wavelengths of the three MLs are 1543.369 nm, 1543.367 nm and 1543.363 nm, respectively. Two optical couplers are used to combine the light beams of the three MLs. Specifically, the light beams from ML2 and ML3 are coupled by a 90:10 optical coupler (OC1), and then the output signal is coupled with that from ML1 by a 50:50 optical coupler (OC2). The powers of MLs are set as 12 dBm, 6 dBm and 6 dBm, respectively. In this case, the injection parameters are  $(f_{i1}, \xi_1) = (4.660 \text{ GHz}, 1.363)$ ,  $(f_{i2}, \xi_2) = (4.912 \text{ GHz}, 0.648)$  and  $(f_{i3}, \xi_3) = (5.416 \text{ GHz}, 0.216)$ . Fig. 6(a) shows the optical spectra of the MLs and SL at the free-running state. Fig. 6(b) shows the optical spectra of signal after optical injection and after OBPF. After optical-to-electrical conversion at a PD, a dual-chirp LFM signal is generated. Fig. 7(a) shows the measured waveform and Fig. 7(b) shows the recovered instantaneous frequency. It is obvious that a dual-chirp LFM signal is successfully generated which has a bandwidth of 6.37 GHz (11.75-18.12 GHz) and a temporal period of 4 ns.

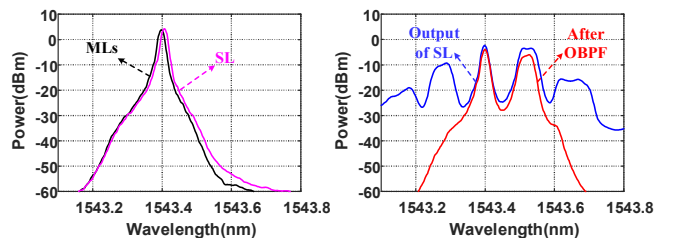


Figure 6. Measured optical spectra of (a) the free-running SL and the MLs, (b) the signal after optical injection and the signal after OBPF when the number of MLs is 3 and the injection parameters are  $(f_{i1}, \xi_1) = (4.660 \text{ GHz}, 1.363)$ ,  $(f_{i2}, \xi_2) = (4.912 \text{ GHz}, 0.648)$  and  $(f_{i3}, \xi_3) = (5.416 \text{ GHz}, 0.216)$ .

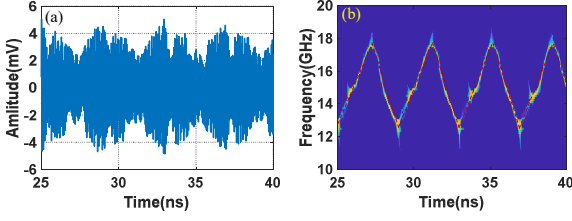


Figure 7. (a) Measured temporal waveform of the generated dual-chirp LFM signal with a bandwidth of 6.37 GHz (11.75-18.12 GHz), and (b) its instantaneous frequency.

#### IV. CONCLUSION

In summary, we have proposed and demonstrated a method for microwave signal generation with reconfigurable frequency-modulation profiles using multi-wavelength P1 dynamics in an optically injected semiconductor laser. Simulations are conducted by solving the modified nonlinear equations and experiments are implemented based on a proof-of-concept system. The generation of microwave signals with different frequency modulation profiles including dual-chirp linear frequency modulation, cosine profile frequency modulation, Gaussian pulse profile frequency modulation and square profile frequency modulation are demonstrated. The results can verify the feasibility of the proposed method, which is expected to find applications in radar, communication and electronic warfare systems.

#### REFERENCES

- [1] H. Kwon and B. Kang, "Linear frequency modulation of voltage-controlled oscillator using delay-line feedback", *IEEE Microw. Wireless Compon. Lett.*, Vol. 15, no. 6, pp. 431–433, Jun. 2005.
- [2] T. Wild, V. Braun, and H. Viswanathan, "Joint Design of Communication and Sensing for Beyond 5G and 6G Systems," *IEEE Access* 9, 30845–30857 (2021).
- [3] F. Zhang, G. Sun, Y. Zhou, B. Gao and S. L. Pan, "Towards High-Resolution Imaging With Photonics-Based Time Division Multiplexing MIMO Radar", *IEEE Journal of Selected Topics in Quantum Electronics*, vol. 28, no. 5, pp. 1-10, Sept.-Oct. 2022.
- [4] F. Zhang, Q. Guo, and S. Pan, "Photonics-based real-time ultra-high-range-resolution radar with broadband signal generation and processing," *Sci. Rep.* Vol. 7, no. 1, pp. 13848, Oct. 2017.
- [5] J. Yao, "Microwave Photonics," *IEEE J. Lightwave Technol.*, vol. 27, no. 3, pp. 314-335, Feb. 2009.
- [6] Q. Guo, F. Zhang, P. Zhou, and S. Pan, "Dual-band LFM signal generation by optical frequency quadrupling and polarization multiplexing," *IEEE Photon. Technol. Lett.*, vol. 29, no. 16, pp. 1320–1323, Aug. 2017.
- [7] Erwin K. Lau, X. Zhao, Hyuk-Kee Sung, Devang Parekh, Connie Chang-Hasnain, and Ming C. Wu, "Strong optical injection-locked semiconductor lasers demonstrating >100-GHz resonance frequencies and 80-GHz intrinsic bandwidths," *Opt. Express.*, Vol. 16, no. 9, pp. 6609-6618, Apr. 2008.
- [8] P. Zhou, F. Zhang, Q. Guo, S. Li, and S. Pan, "Reconfigurable radar waveform generation based on an optically injected semiconductor laser," *IEEE J. Sel. Topics Quantum Electron.*, vol. 23, no. 6, pp. 1801109- 1–9, Nov. 2017.
- [9] G. Sun, F. Zhang, and S. Pan, "Millimeter-level resolution through the-wall radar imaging enabled by an optically injected semiconductor laser," *Opt. Lett.*, vol. 46, no. 22, pp. 5659-5662, Nov. 2021.
- [10] X. Yu, G. Sun, F. Zhang, and S. Pan, "Frequency-modulated microwave signal generation by dual-wavelength-injection period-one laser dynamics," *Opt. Lett.* Vol. 47, no. 22, pp. 5921-5924, Nov. 2022.
- [11] S. C. Chan, "Analysis of an optically injected semiconductor laser for microwave generation," *IEEE J. Quantum Electron.* Vol. 46, no. 3, pp. 421–428, Feb. 2010.
- [12] S. Hwang, J. Liu and J. White, "35-GHz intrinsic bandwidth for direct modulation in 1.3- $\mu\text{m}$  semiconductor lasers subject to strong injection locking," *IEEE Photonics Technol. Lett.*, vol. 16, no. 4, pp. 972-974, Apr. 2004.
- [13] J. W. Shi, F. M. Kuo, N. W. Chen, S. Y. Set, C. B. Huang, and J. E. Bowers, "Photonic generation and wireless transmission of linearly/nonlinearly continuously tunable chirped millimeter-wave waveforms with high time bandwidth product at W-band," *IEEE Photonics J.* Vol. 4, no. 1, pp. 215–223, Jan. 2012.